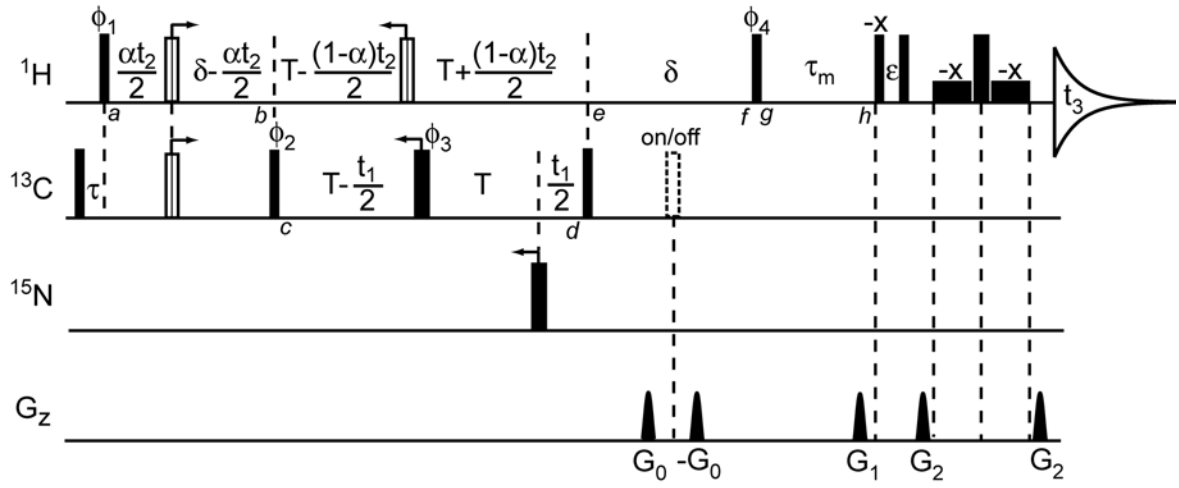

Figure 1S. 3D CT-HMQC-IPAP-NOESY pulse sequence. Narrow and wide filled bars represent 90° and 180° pulses, respectively. Use of composite pulses (vertically hatched open bars: $90°_x200°_y90°_x$ for ^{1}H and $90°_x220°_y90°_x$ for ^{13}C) reduces resonance offset and RF inhomogeneity effects. The 180° ^{13}C pulse depicted by the dashed open bar is applied only when acquiring the anti-phase (AP) spectrum, but replaced with a delay of identical duration for the interleaved acquisition of the in-phase (IP) spectrum. The two gradient pulses of opposite polarity flanking the 180° ^{13}C pulse serve to suppress off-resonance artifacts. Delays: τ = 50 ms, δ = 3 ms, T = 12.5 ms, τ_m = 40 ms; ^{13}C carrier position: 74.2 ppm. The 90_{-x}-ε-90_x module[15] is optimized for detection of the 2′OH proton resonances centered at 6.8 ppm ($\varepsilon \approx 170$ μs at 800 MHz). The low power $90°_{-x}$ ^{1}H pulses of the WATERGATE scheme[11] have durations of 1.5 ms. All pulses have phase x unless otherwise stated. Phase cycling: ϕ_1 and ϕ_2 = x + States-TPPI; ϕ_3 = x, y, -x, -y; ϕ_4 = y (AP) or –x (IP); receiver = x, -x. Spectral widths: F_1, 20.9 ppm; F_2, 2.1 ppm; α = 0.2. Pulsed field z gradients are sine-bell shaped with durations of 1 ms (G_0), 2.1 ms (G_1) and 350 μs (G_2), using peak amplitudes 3, 19.8, and 30 G cm^{-1}, respectively. Processing scripts and Bruker pulse sequence code can be downloaded from http://spin.niddk.nih.gov/bax/.

Analysis of the CT-HMQC-IPAP-NOESY pulse sequence in terms of product operator formalism, for the case of an isolated ^{13}C-^{1}H group in NOE contact with an OH proton. Only terms at various points in the sequence that contribute to the final observed signal are included, and only the first step of the phase cycle is considered ($\phi_1 = \phi_2 = x$).

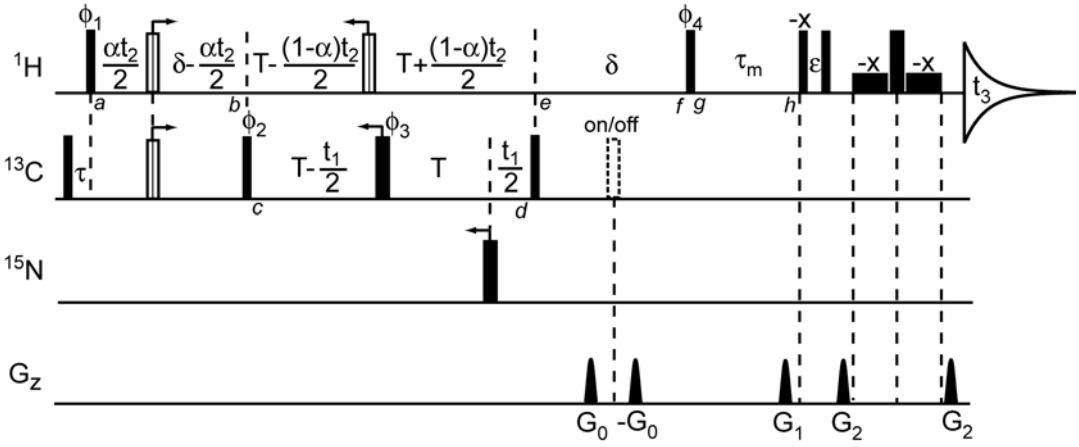

a: $-H_y$

b: $2H_xC_z \cos[\omega_H(\alpha t_2-\delta)] - 2H_yC_z \sin[\omega_H(\alpha t_2-\delta)]$

c: $-2H_xC_y \cos[\omega_H(\alpha t_2-\delta)] + 2H_yC_y \sin[\omega_H(\alpha t_2-\delta)]$

d: $-2H_xC_y \cos[\omega_C t_1]\cos[\omega_H(t_2-\delta)] - 2H_yC_y \cos[\omega_C t_1]\sin[\omega_H(t_2-\delta)]$

e: $-2H_xC_z \cos[\omega_C t_1]\cos[\omega_H(t_2-\delta)] - 2H_yC_z \cos[\omega_C t_1]\sin[\omega_H(t_2-\delta)]$

f: $-H_y \cos[\omega_C t_1]\cos[\omega_H t_2]$ (IP, when the 180° ^{13}C pulse is off)

$2H_xC_z \cos[\omega_C t_1]\cos[\omega_H t_2]$ (AP, when the pulse is on)

g: $H_z \cos[\omega_C t_1]\cos[\omega_H t_2]$ (IP)

$-2H_zC_z \cos[\omega_C t_1]\cos[\omega_H t_2]$ (AP)

h: $OH_z \cos[\omega_C t_1]\cos[\omega_H t_2] + H_z \cos[\omega_C t_1]\cos[\omega_H t_2]$ (IP)

$-2OH_zC_z \cos[\omega_C t_1]\cos[\omega_H t_2] - 2H_zC_z \cos[\omega_C t_1]\cos[\omega_H t_2]$ (AP)

Correction factors for the intensity reduction of NOEs from various ribose protons to the 2′OH proton resulting from passive couplings during the constant-time evolution periods in Figure 1 are empirically determined as follows:

A number of well resolved ^{13}C-dispersed NOE diagonal peaks of H1′, H2′, H3′, and H4′ are selected in the in-phase spectrum of 3D CT-HMQC-IPAP-NOESY. In *F3*, these diagonal peaks are split by the $^{1}J_{CH}$ couplings. Only the more intense doublet component with a larger offset from the carrier frequency is used to derive the correction factors. Intensity attenuation of each selected peak resulting from the excitation profiles of the Jump-Return and WATERGATE detection elements are first corrected on the basis of the intensity reduction experimentally observed for the CH_3 peak in the 1D ^{1}H spectrum of sodium acetate in D_2O (acquired as a function of resonance offset, using the same Jump-Return and WATERGATE settings as used in Figure 1S). The excitation-profile-corrected diagonal NOE intensities are then averaged for each type of ribose proton. The correction factors for the effect of passive couplings are then calculated as the ratios of the averaged H1′ diagonal intensity to the averaged H2′, H3′, and H4′ diagonal intensities, respectively. As a result, a correction factor relative to H1′-2′OH is obtained for each type of ribose proton, because the absolute NOE intensity for each type of protons is unknown and modulated by hydrogen exchange. Such relative correction factors suffice because only the relative NOE intensities are used in the analysis of the 2′OH orientations. The correction factors for the effect of passive couplings on peak intensities are given below, and have been used to scale up the observed NOE cross peak intensities from each type of ribose proton to the 2′OH proton in the in-phase spectrum of 3D CT-HMQC-IPAP-NOESY.

C1′-H1′: 1.0

C2′-H2′: 1.8 ± 0.3

C3′-H3′: 3.5 ± 0.2

C4′-H4′: 2.5 ± 0.4

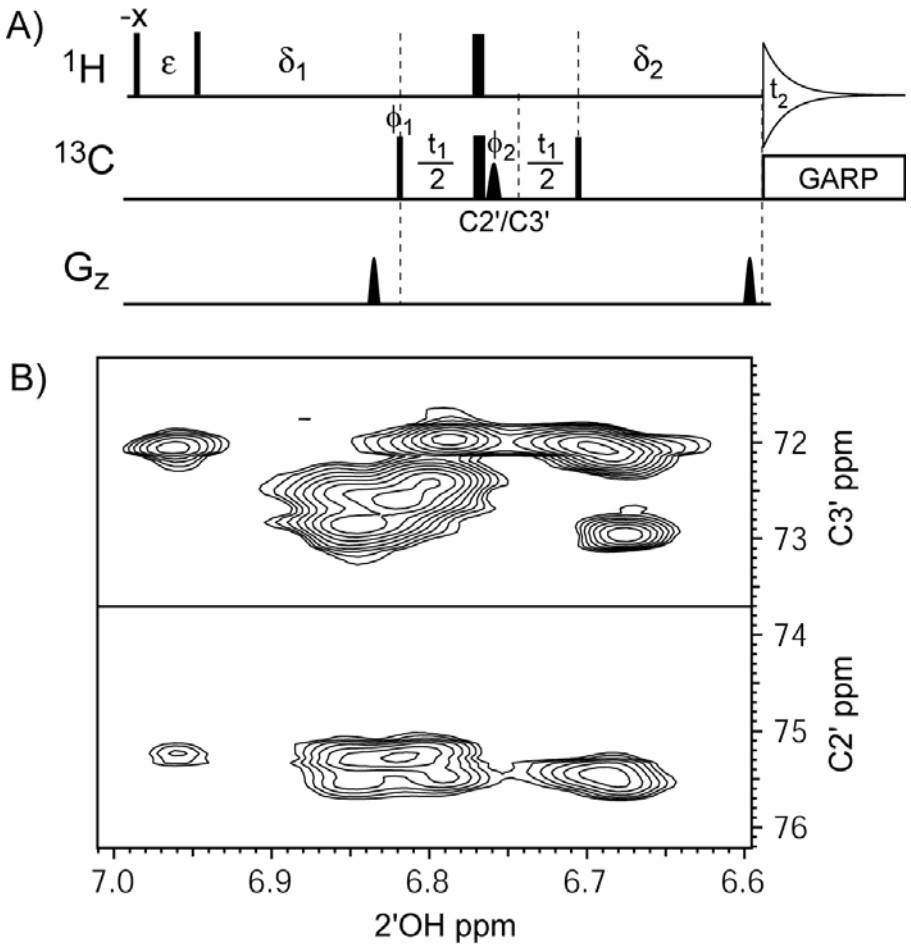

Figure 2S. A) Quantitative HMBC pulse sequence for measurement of $^{3}J_{C3'\text{-}2'OH}$, using the $^{2}J_{C2'\text{-}2'OH}$ values obtained from 3D CT-HMQC-IPAP-NOESY as an internal reference. Narrow and wide bars represent 90° and 180° pulses, respectively. The 180° C2′/C3′ shaped pulse has the REBURP profile (Geen and Freeman, *J. Magn. Reson.* **1991**, *93*, 93-141), duration of 3 ms, and are centered at 78.9 and 70.0 ppm for C2′ and C3′ respectively. Delay duration: ε = 160 μs; δ_1 = 18 ms; δ_2 = 18 ms - pw, where pw is the duration of the REBURP pulse; the delay between transients = 600 ms. All pulses have phase x unless otherwise stated. Phase cycling: ϕ_1 = 4(x), 4(-x) + States-TPPT; ϕ_2 = x, y, -x, -y; receiver = 2(x, -x), 2(-x, x).

B) Selected regions of two HMBC spectra, acquired at 6 °C and 800 MHz with a cryogenic triple resonance probehead. The spectra were processed and analyzed using NMRPipe (Delaglio et al. *J. Biomol. NMR* **1995,** *6*, 277-293), and are displayed at the same contour level. The intensities of overlapping cross peaks were deconvoluted using the non-linear spectral fitting routine within the NMRPipe software package, with fixed peak positions (obtained from other types of spectra) and line width (estimated from resolved peaks) in both dimensions. The following equation was solved numerically to obtain $^{3}J_{C3'\text{-}2'OH}$:

$$I_{C3'} / I_{C2'} = \tan(\pi\, {}^{3}J_{C3'\text{-}2'OH}\, \delta_1)\, \tan(\pi\, {}^{3}J_{C3'\text{-}2'OH}\, \delta_2) / \tan(\pi\, {}^{2}J_{C2'\text{-}2'OH}\, \delta_1)\, \tan(\pi\, {}^{2}J_{C2'\text{-}2'OH}\, \delta_2)$$

where $I_{C3'}$ and $I_{C2'}$ are the peak intensities for C3′-2′OH and C2′-2′OH, respectively.

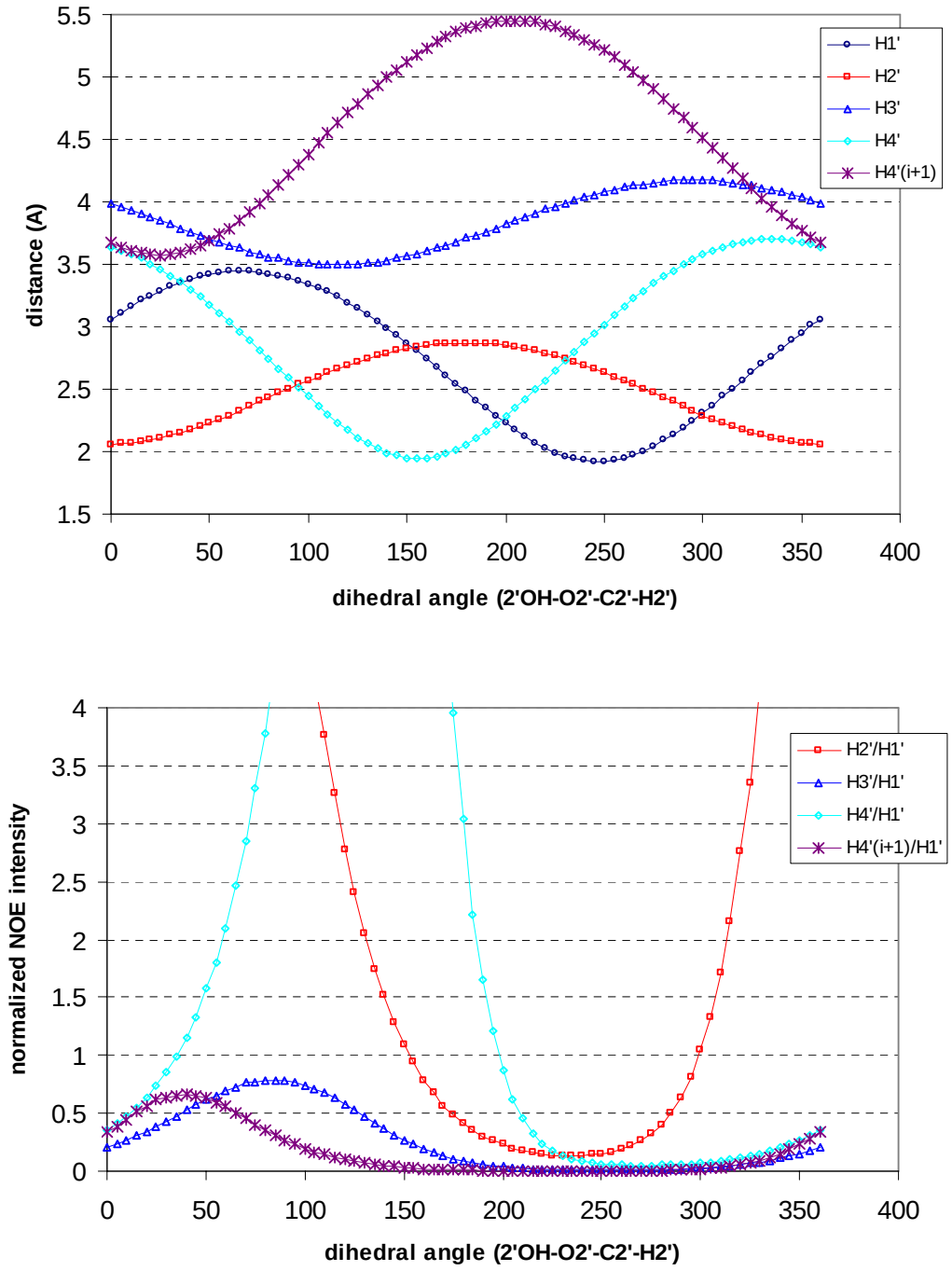

Figure 3S. Plot of distances between 2′OH and other intra-nucleotide and sequential ribose protons as a function of the 2′OH orientation (upper panel) and NOE intensity between the 2′OH and other ribose protons normalized to those between the 2′OH intra-nucleotide H1′ protons (lower panel). All the calculations were performed using a high resolution RNA crystal structure (PDB code: 256D, reference 2, main text).

Table 1S. Solvent exchange rates of the 2′OH protons with bulk water at 6 °C, measured by selectively pre-inverting the 2′OH peaks followed by a variable delay and a water-flip-back NOESY readout.

nucleotide	solvent exchange rate (s^{-1})
G738	52 ± 5
G739	39 ± 1
C740	21 ± 3
U741	33 ± 2
A742	31 ± 1
A743	39 ± 1
U754	35 ± 15
U755	37 ± 2
G757	29 ± 2
C758	18 ± 4
C759	33 ± 2
C760	120 ± 40

Table 2S. Coupling constants (Hz) between the 2′OH and the C1′, C2′, and C3′ ribose carbons.

	C1'[a]	C2'[a]	C3'[b]
G738	3.7 ± 1.0[c]	-3.3 ± 0.6	4.0 ± 0.8
G739	1.0 ± 0.4	-2.3 ± 0.3	3.3 ± 0.3
C740	0.9 ± 0.4	-2.5 ± 0.3	4.4 ± 0.4
U741	2.6 ± 0.5	-2.5 ± 0.4	4.5 ± 0.6
A742	1.5 ± 0.5	-2.3 ± 0.3	3.8 ± 0.4
A743	1.1 ± 0.5	-2.4 ± 0.6	4.4 ± 0.8
U754	0.8 ± 0.6	-2.2 ± 0.4	3.4 ± 0.5
U755	2.0 ± 0.7	-3.0 ± 0.5	5.7 ± 0.8
G757	0.8 ± 0.3	-2.6 ± 0.3	4.7 ± 0.4
C758	1.8 ± 0.3	-2.4 ± 0.4	3.8 ± 0.5
C759	0.5 ± 0.4	-2.4 ± 0.4	3.9 ± 0.5
C760	2.3 ± 1.6	-3.3 ± 0.9	n.a.[d]

[a] Couplings measured from the CT-HMQC-IPAP-NOESY discussed in the text.
[b] Couplings measured from the J-modulated HMBC spectra. Two measurements were made and the averaged values are reported in the table. The reported error includes propagation of the error in the $^3J_{C2'\text{-}2'OH}$ coupling.
[c] Coupling not used in the analysis because it is inconsistent with the very weak intensity of the HMBC cross peak.
[d] Coupling not available due to the unobservable HMBC cross peaks, caused by the fast OH exchange rate of C760.

Table 3S. Normalized intensities of NOEs between the 2′OH proton and the H2′, H3′, and H4′ protons, relative to the NOE intensity from the 2′OH proton to the intra-ribose H1′ proton, obtained from the constant-time HMQC-IP-NOESY measurement (Figure 4S) as described in the text. All the NOE intensities have been adjusted using the correction factors given in the text to account for the effect of the passive couplings during the t_1 and t_2 evolution periods.

nucleotide	H2′ intra-nucleotide	H3′ intra-nucleotide	H4′ intra-nucleotide	H4′ sequential
G738	2.9 ± 0.3	< 0.32[a]	< 0.23[a]	< 0.23[a]
G739	2.3 ± 0.1	0.25 ± 0.05	0.25 ± 0.05	< 0.1[a]
C740	2.1 ± 0.1	0.30 ± 0.05	0.20 ± 0.05	< 0.1[a]
U741	2.4 ± 0.1	0.4 ± 0.1	0.35 ± 0.05[b]	0.2 ± 0.1
A742	3.5 ± 0.2	0.4 ± 0.1	0.5 ± 0.1	< 0.13[a]
A743	1.7 ± 0.1	< 0.18[a]	0.2 ± 0.1	< 0.13[a]
U754	2.5 ± 0.2	0.3 ± 0.1	0.3 ± 0.1	< 0.13[a]
U755	2.6 ± 0.2	0.4 ± 0.1	0.35 ± 0.05[b]	< 0.15[a]
G757	1.6 ± 0.1	0.20 ± 0.05	0.20 ± 0.05	< 0.1[a]
C758	1.6 ± 0.1	< 0.1[a]	0.20 ± 0.05	< 0.1[a]
C759	1.7 ± 0.1	0.25 ± 0.05	0.30 ± 0.05	< 0.1[a]
C760	3.6 ± 0.1	1.1 ± 0.1	< 0.4	< 0.4

[a] No NOE peak is detected in the in-phase spectrum of the 3D CT-HMQC-IPAP-NOESY spectrum. The upper limit intensity is estimated from the NOE intensity being below three times the rms spectral noise.

[b] Averaged intensity of overlapping cross peaks, assuming they are equal.

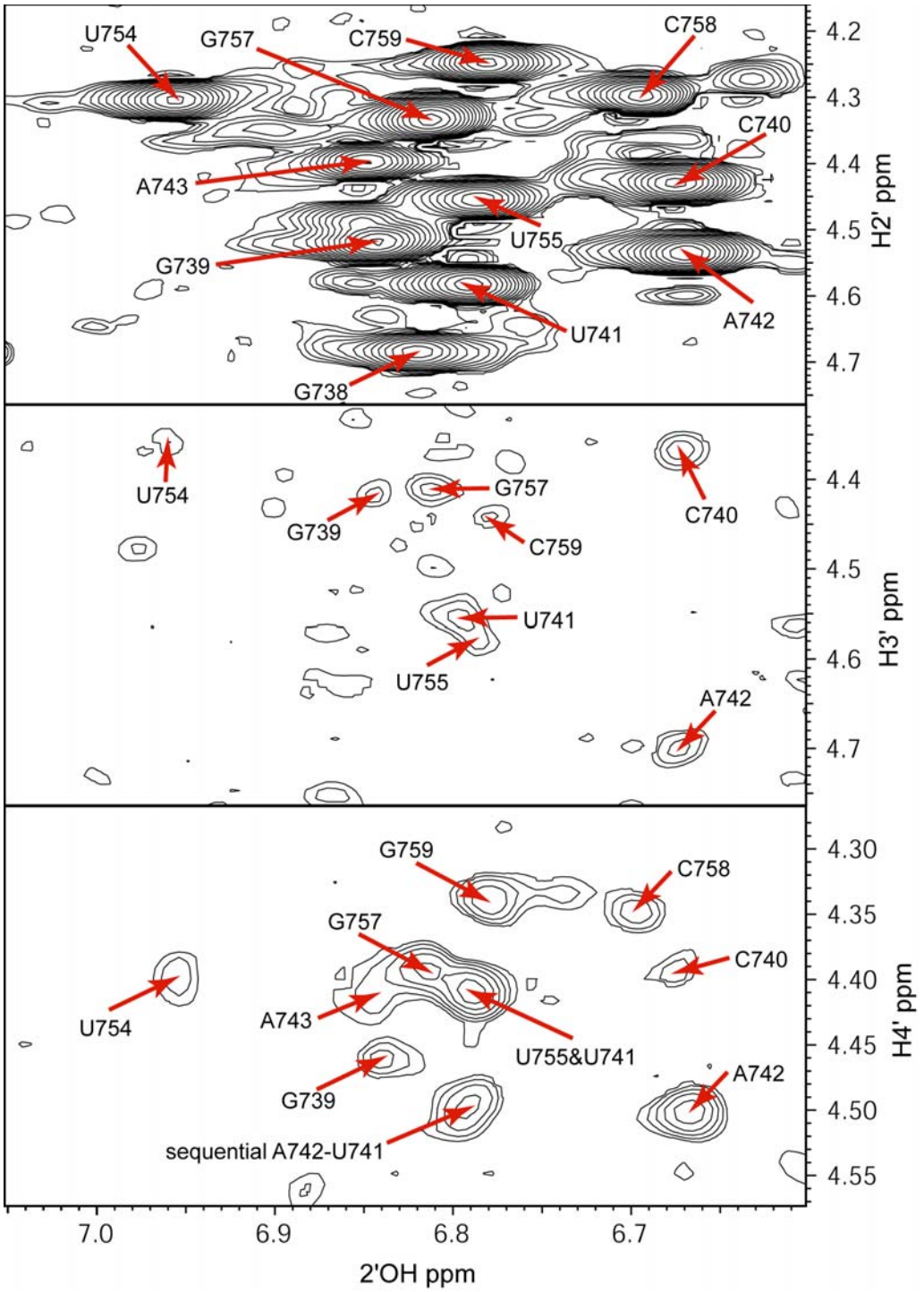

Figure 4S. 2D skyline projections of selected ^{13}C regions (top 75.0-75.8 ppm for C2', center 71.8-72.9 ppm for C3', bottom 81.4-82.2 ppm for C4') of the 3D HMQC-IP-NOESY spectrum (data acquisition time: 41 hours; NOE mixing time: 40 ms) using the pulse sequence shown in Figure 1. All panels are drawn at an identical contour level and using the same contour multiplier of 1.25.

Table 4S. Normalized intensities of NOEs between the 2′OH proton and the H2′, H3′, and H4′ protons, relative to the NOE intensity from the 2′OH proton to the intra-ribose H1′ proton, obtained from the constant-time 3D HSQC-NOESY measurement (Figure 5S).

nucleotide	H2′ intra-nucleotide	H3′ intra-nucleotide	H4′ intra-nucleotide	H4′ sequential
G738	2.3 ± 0.5	< 0.21[a]	< 0.21[a]	< 0.21[a]
G739	2.2 ± 0.3	0.2 ± 0.1	0.3 ± 0.1	< 0.1[a]
C740	1.9 ± 0.2	0.17 ± 0.08	0.33 ± 0.09	< 0.09[a]
U741	2.1 ± 0.2	0.3 ± 0.1	0.33 ± 0.08[b]	0.2 ± 0.1
A742	2.8 ± 0.3	< 0.12[a]	0.3 ± 0.1	< 0.12[a]
A743	1.6 ± 0.2	< 0.11[a]	0.3 ± 0.1	< 0.11[a]
U754	1.9 ± 0.2	< 0.1[a]	0.2 ± 0.1	< 0.1[a]
U755	2.1 ± 0.3	0.2 ± 0.1	0.33 ± 0.08[b]	< 0.13[a]
G757	1.21 ± 0.08	0.13 ± 0.05	0.26 ± 0.06	< 0.1[a]
C758	1.3 ± 0.1	0.14 ± 0.06	0.21 ± 0.07	< 0.1[a]
C759	1.4 ± 0.1	0.19 ± 0.07	0.26 ± 0.08	< 0.1[a]
C760	3.1 ± 1.0	< 0.33[a]	< 0.33	< 0.33

[a] No NOE peak is detected in the 3D CT-HSQC-NOESY spectrum. The upper limit intensity is estimated from the NOE intensity being below three times the rms spectral noise.

[b] Averaged intensity of overlapping cross peaks, assuming they are equal.

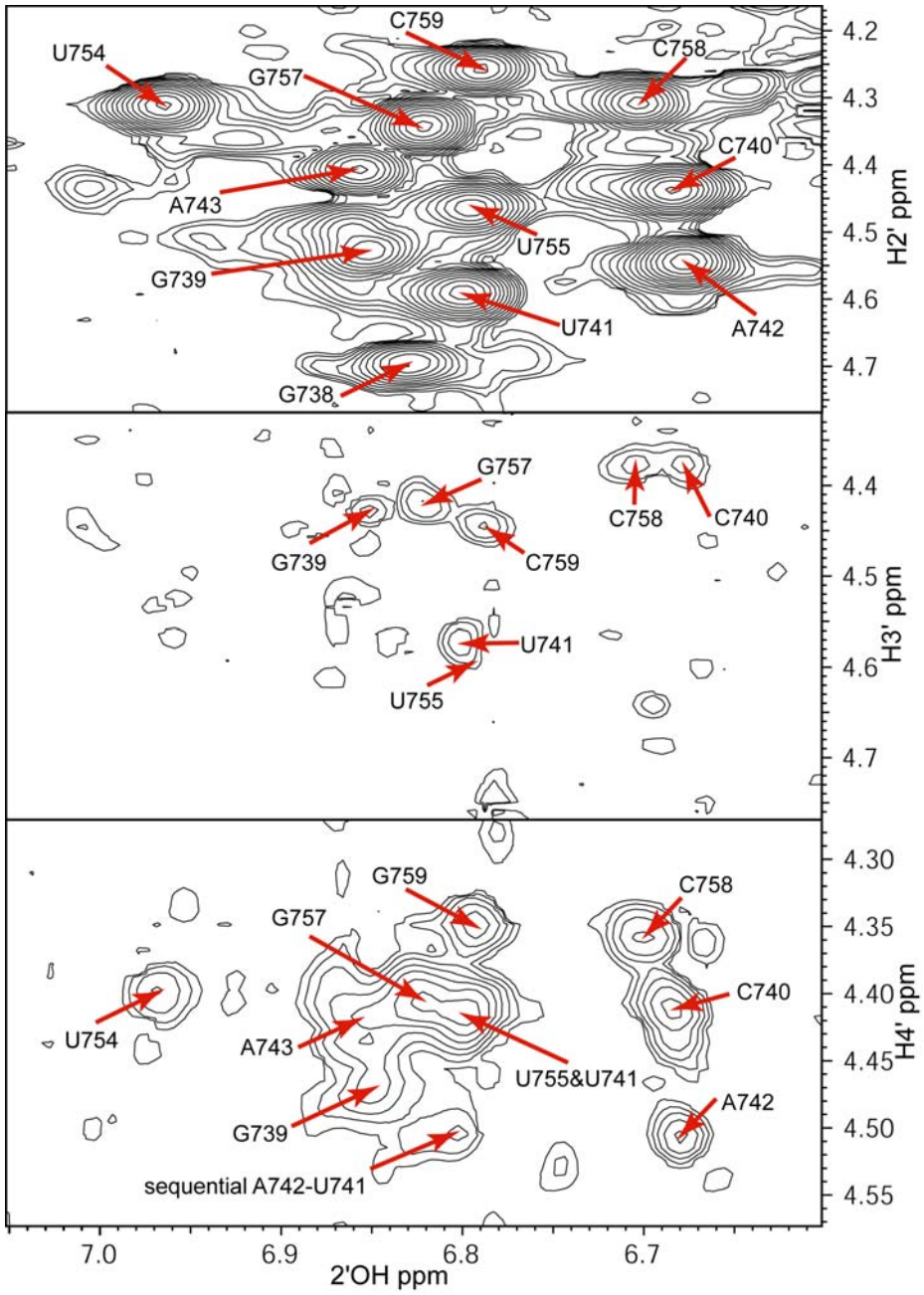

Figure 5S. 2D skyline projections of selected ^{13}C regions (top 75.0-75.8 ppm for C2', center 71.8-72.9 ppm for C3', bottom 81.4-82.2 ppm for C4') of the constant-time 3D HSQC-NOESY spectrum (data acquisition time: 43 hours; NOE mixing time: 40 ms). The pulse sequence starts from INEPT transfer from ribose protons to carbons, whose magnetization is then labeled during a 25-ms constant time delay. The magnetization is then transferred back to the ribose protons, followed by a semi-constant-time type of rephasing as well as ^{1}H chemical shift encoding. After the 40-ms NOE mixing, the magnetization is then detected in the same way as described in Figure 1. All panels are drawn at an identical contour level and using the same multiplier of 1.25.